Nano-scale photonic crystal microcavity characterization with an all-fiber based 1.2 – 2.0 μm supercontinuum

Peter T. Rakich, Hideyuki Sotobayashi*, Juliet T. Gopinath, Steven G. Johnson, Jason W. Sickler, Chee Wei Wong†, John D. Joannopoulos, and Erich P. Ippen

Research Laboratory of Electronics, Massachusetts Institute of Technology, Cambridge MA 02139, USA
** also with National Institute of Information and Communication Technology, Tokyo, JAPAN*
†Mechanical Engineering, Columbia University, New York, NY 10027
rakich@mit.edu

Abstract: The use of ultra-broadband supercontinuum generated by an all-fiber system to characterize high-index contrast photonic circuits over the wavelength range 1.2 – 2.0 μm is demonstrated. Efficient, broadband waveguide coupling techniques and sensitive normalized detection enable rapid and high-resolution measurements of nano-scale one-dimensional photonic crystal microcavities. Experimental mappings of bandgaps and cavity mode resonances with a wavelength resolution of 0.1 nm compare well with computer simulations.

OCIS codes: (190.4370) Nonlinear optics, fiber; (320.7110) Ultrafast nonlinear, ultrafast lasers; (302.7090) Waveguides; (250.5300) Photonic Integrated Circuits

References and links

1. J.S. Foresi, P.R. Villeneuve, J. Ferrera, E.R. Thoen, G. Steinmeyer, S. Fan, J.D. Joannopoulos, L.C. Kimerling, H.I. Smith, and E.P. Ippen, "Photonic-bandgap microcavities in optical waveguides," Nature **390**, 143 (1997).
2. C. Luo, S.G. Johnson, J.D. Joannopoulos, and J.B. Pendry, "Subwavelength imaging in photonic crystals," Phys. Rev. B, **65**, 201104 (2002).
3. R.T. Neal, M.D.C. Charlton, G.J. Parker, C.E. Finlayson, M.C. Netti, and J.J. Baumberg, "Ultrabroadband transmission measurements on waveguides of silicon-rich silicon dioxide," Appl. Phys. Lett. **83**, 4598 (2003).
4. M.C. Netti, C.E. Finlayson, J.J. Baumberg, M. Charlton, M. Zoorob, J. Wilkinson, and G. Parker, " Separation of photonic crystal waveguides modes using femtosecond time-of-flight" Appl. Phys. Lett. **81**, 3927 (2002).
5. M. Qi, E. Lidorikis, P.T. Rakich, S.G. Johnson, J.D. Joannopoulos, E.P. Ippen, and H.I. Smith, "A three-dimensional optical photonic crystal with designed point defects" Nature **429**, 538 (2004).
6. Y. Kuroiwa, N. Sugimoto, K. Ochiai, S. Ohara, Y. Fukasawa, S. Ito, S. Tanabe, and T. Hanada, "Fusion spliceable and high efficient Bi_2O_3-based EDF for short length and broadband amplification pumped at 1480 nm," *Proc. 26th Optical Fiber Communication Conference*, Post Conference Edition, Vol. 2 of OSA Proceedings Series (Optical Society of America, Washington, D.C., 2001), pp. TuI5-1-3.
7. H.A. Haus, K. Tamura, L.E. Nelson, and E.P. Ippen, "Stretched-pulse additive pulse mode-locking in fiber ring lasers: theory and experiment," IEEE J. Quant. Electron. **31**, 591 (1995).
8. K. Shiraishi, H. Hatakeyama, H. Matsumoto, and K. Matsumura, "Laminated polarizers exhibiting high performance over a wide range of wavelength," J. Lightwave Technol. **15,** 1042-50 (1997).
9. S.G. Johnson and J.D. Joannopoulos, "Block-iterative frequency-domain methods for Maxwell's equations in a planewave basis," Opt. Express **8**, 173-190 (2001).
10. K.S. Kunz and R.J. Luebbers, "The finite-difference time-domain method for electromagnetics," (CRC Press: Boca Raton, 1993).
11. M.A. Kaliteevski, J. Manzanares Martinez, D. Cassagne, and J.P. Albert, "Block-iterative frequency-domain methods for Maxwell's equations in a planewave basis," Phys. Rev. B **66**, 113101 (2002).

#6001 - $15.00 US Received 9 December 2004; revised 21 January 2005; accepted 23 January 2005

1. Introduction

High-index contrast (HIC) photonic crystal waveguides are of interest for a variety of applications such as integrated photonic circuits, quantum optics, and super resolution [1,2]. However, the measurements required to understand basic physical phenomena of photonic crystal devices often present serious experimental challenges. In many cases it is necessary to perform spectral measurements over 50 - 100% of the center frequency of the device (i.e. as much as an octave) in order to understand the bandgap-related phenomena, which are often difficult to distinguish from other optical phenomena when measured over a narrow bandwidth. Conventional measurement techniques employ tunable lasers to scan the broad spectral features of photonic crystals. However, tunable sources that span the entire 1 - 2 μm spectral range, critical for the characterization of broadband photonic devices centered at telecommunications wavelengths, are not readily available.

In this paper a fiber laser-based supercontinuum (SC) source is demonstrated and used to characterize nano-scale photonic crystal waveguides over the spectral range 1.2 - 2.0 μm. Previous work has used SC centered at 800 nm to measure two-dimensional photonic crystal slab waveguides with a system utilizing free space optics [3,4]. In contrast, this work uses a SC source centered at telecommunications wavelengths (1.55 μm) and an all-fiber measurement apparatus that optimizes nano-scale coupling and collection efficiencies, reducing the required SC power. This new approach is used to study HIC one-dimensional (1-D) photonic crystal microcavities with high fidelity measurements of the photonic bandgaps and microcavity resonances. Similar methods to those described here were recently applied to the study of three-dimensional photonic crystals with point defects [5].

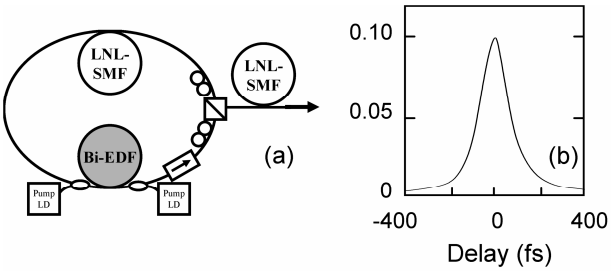

Fig. 1. (a) Diagram of fiber laser consisting of bi-directionally pumped segment of Bi-EDF fiber and LNL-SMF. A length to LNL-SMF is used to compress the pulses to 100 fs. (b) An autocorrelation of the laser pulses after compression.

2. Supercontinuum source

The SC source consists of a length of highly nonlinear dispersion-shifted fiber (HNL-DSF) seeded by a femtosecond stretched-pulse fiber laser, shown in Fig. 1(a). The laser consists of a 55.6 cm length of bismuth oxide-based erbium-doped fiber (Bi-EDF), 1.8 m of low-nonlinearity single-mode fiber (LNL-SMF), two polarization controllers, and a polarizing beam-splitter. The output is taken from the rejection port of the polarizing beam splitter. The 55.6 cm length of Bi-EDF has a broad gain bandwidth and high gain per unit length [6]. It has an erbium concentration of 6470 wt. ppm and is bi-directionally pumped with two 975 nm laser diodes. To balance the dispersion of the Bi-EDF, 1.8 m of LNL-SMF (group-velocity dispersion of 20.64 ps/nm/km at 1550 nm) is included. Mode-locked operation is obtained through nonlinear polarization rotation [7]. The center wavelength of the laser output is 1571 nm, the spectral width is 58 nm, and the repetition rate is 34.18 MHz. For pump powers of 350 mW, the laser output power is 28 mW. The pulse width at the output is 1.57 ps but can be externally compressed to 100 fs with 1.8 m of LNL-SMF. The autocorrelation of the compressed pulses is shown in Fig. 1(b). Although the pulse width obtained is approximately 50% greater than transform limited, a peak power of 8.5 kW enables the generation of high quality SC spectrum. Pulses are injected into 500 m of HNL-DSF having a zero-dispersion

#6001 - $15.00 US Received 9 December 2004; revised 21 January 2005; accepted 23 January 2005

wavelength of 1565 nm and a nonlinear coefficient of 21 km^{-1} W^{-1} to generate SC. The laser spectra before and after the HNL-DSF are shown in Fig. 2(b).

3. Experimental setup

The SC spectrum generated in the HNL-DSF is coupled into an apparatus, shown in Fig. 2(a), for waveguide transmission studies. SC light is first passed through a broadband fiber-optic coupler, splitting the continuum into two ports, signal and reference. The signal is passed through the waveguide while the reference is used to normalize fluctuations and spectral variations from the SC source. The signal is then sent through an integrated polarizer and polarization controller to define the input polarization and is then coupled into the waveguide with a lensed fiber. A second lensed fiber collects the waveguide output that is sent through a polarization controller and integrated polarizer for polarization analysis.

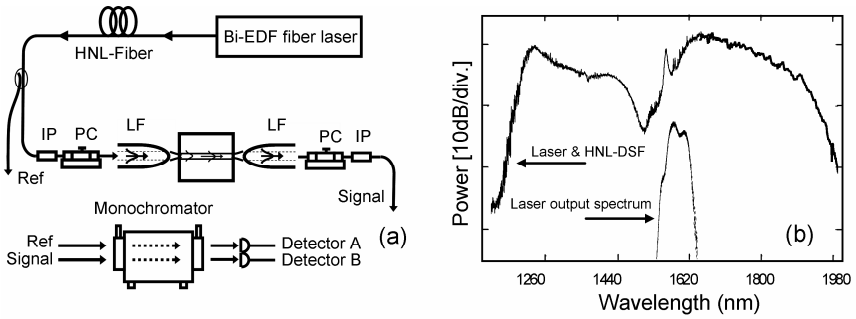

Fig. 2. (a) A schematic of measurement apparatus. A small fraction of SC light is diverted by a coupler for reference (Ref) measurement while the remainder (Signal) is passed through the waveguide. (b) spectrum at fiber laser output (dotted) and a characteristic SC spectrum generated by the HNL-DSF (solid). The apparent roll-off of SC spectrum at 2 μm is due to decreasing photodetector response. The SC spectral measurement was taken with optical spectrum analyzer (1150 - 1700 nm) and spectrometer (1700 - 1980 nm).

By imaging the signal and the reference through a monochromator onto two identical photodetectors, normalization of the fluctuations in the SC spectrum is performed. Peltier-cooled IR-enhanced InGaAs photodiodes and lock-in detection are used to achieve low noise measurements (with a noise equivalent power of 28 fW/√Hz) and enable rapid scans (less than one minute) with as little as 4 mW of SC light. Polarization control of the light launched into the waveguide and polarization analysis of the light collected from the guide is performed with broadband integrated polarizers and strain-type polarization controllers, providing greater than 20 dB of polarization extinction over nearly the entire spectral range [8]. In addition, lensed fibers provide efficient coupling and collection over the entire wavelength range.

4. Photonic crystal under study

The SC source and measurement apparatus were applied to a number of HIC devices [5]. However, the device examined in this study is a 1-D photonic bandgap microcavity [1]. It consists of a silicon strip on top of an oxide layer, forming a single-mode waveguide with only a TE-like mode. The photonic crystal was formed by etching a periodic array of holes through the waveguide. The microcavity defect was defined by increasing one hole spacing from a (the lattice constant) to a_d (the defect length). The device schematic and scanning electron micrograph (SEM) are shown in Fig. 3(b). For comparison, simulations of the device band structure [9] and transmission [10] were performed using the parameters extracted from SEM measurements.

Simulations and experimental results are shown in Fig. 3(c). The lattice constant, a, found through SEM measurements is 424 nm ± 5%. Simulations agree best with the measured

#6001 - $15.00 US Received 9 December 2004; revised 21 January 2005; accepted 23 January 2005

spectrum when using a = 410 nm, which is within the experimental uncertainty; no other parameters were adjusted.

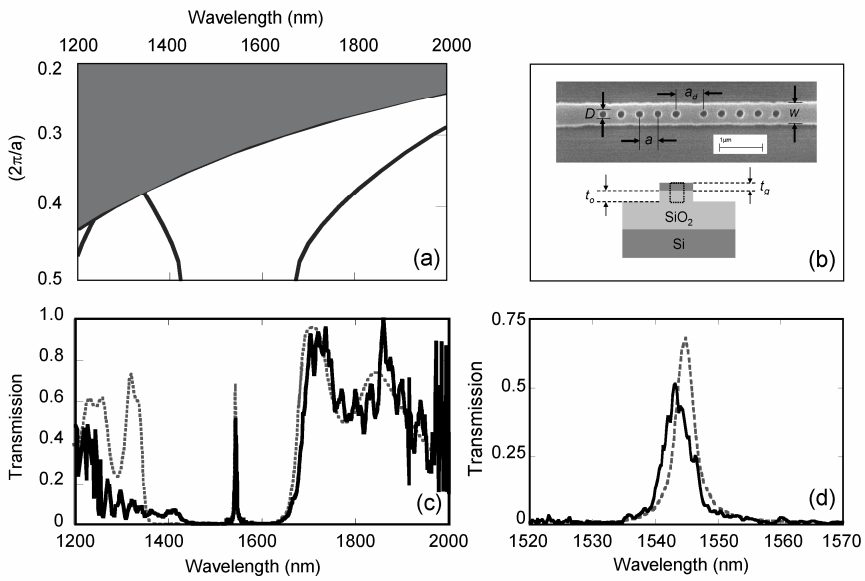

Fig. 3. (a) Band diagram (TE-like bands only) based on SEM measurements of device. Grey region indicates states above the light line. (b) SEM of microcavity (top) and cross-section of waveguide (bottom). Device parameters extracted from SEM are a = 424 nm, a_d = 649 nm, w = 494 nm, t_g = 195 nm, t_o = 350 nm, and D = 179 nm. (c) A transmission measurement (solid) and simulated transmission (dashed) of photonic crystal microcavity (TE polarization). The transmission measurement is normalized to that of a similar waveguide without etched holes. (d) High resolution (0.1 nm) measurement (solid) and simulation (dashed) of the microcavity resonance.

Remarkable agreement is seen between experiment and theory. A 265 nm stop-band is clearly visible in the experiment from approximately 1425 - 1690 nm. In addition, a sharp microcavity resonance can be seen at 1542 nm, demonstrating efficient power coupling through the photonic crystal, with approximately 52% transmission. This is in good agreement with the simulated transmission efficiency of 68%. The computed band structure, seen in Fig 3(a), predicts a bandgap from 1400 - 1670 nm, which is also seen in the experimental data.

It is worth noting that experiment and simulation diverge at wavelengths below ~1400 nm. These shorter wavelength modes lie within the "air-band", which leads to increased sensitivity to roughness and disorder [11]. These result in increased losses for the TE mode and coupling to higher order modes, and cause the discrepancy.

Another key performance characteristic of this device is the microcavity quality factor (Q), which requires a high resolution measurement. In performing high resolution measurements, the major limitation is the finite spectral power-density of the SC source. Nevertheless, with the fiber laser-based SC source, 0.1 nm resolution measurements of the microcavity were performed. These results are shown in Fig. 3(c). A Lorentzian fit of the microcavity resonance yields a spectral width of 4.4 nm, demonstrating a microcavity Q of approximately 350 which is in reasonable agreement with the simulated Q of 480, despite the disorder present in the device.

#6001 - $15.00 US Received 9 December 2004; revised 21 January 2005; accepted 23 January 2005

5. Conclusion

In conclusion, a novel SC-based white-light source is developed and its utility for performing high-fidelity optical transmission measurements of waveguides and photonic crystals over broad spectral ranges in the near-IR is demonstrated. A compact stretched-pulse mode-locked fiber laser source is used to generate continuum radiation spanning the range 1.2 - 2.0 μm. Modest levels of continuum light (4 mW) are found to be sufficient to perform broadband transmission measurements of nano-scale waveguides and photonic crystal microcavities when sensitive detection techniques, efficient polarization control, and waveguide coupling methods are employed. This newly developed measurement method enables precise measurement of the photonic bandgap wavelengths and attenuation factors of 1-D photonic crystal microcavities. In addition, high resolution measurements (0.1 nm) make spectral measurements of microcavity modal frequencies and quality factors possible.

Acknowledgments

The authors gratefully acknowledge Minghao Qi, Benjamin Barbrel, Tymon Barwicz, Poh-Boon Phua, and Milos Popovic for valuable discussion and technical contributions, as well as AFOSR, NSF, and MRSEC for funding.

#6001 - $15.00 US Received 9 December 2004; revised 21 January 2005; accepted 23 January 2005